

**NEUROMODELING OF MICROWAVE CIRCUITS EXPLOITING
SPACE MAPPING TECHNOLOGY**

J.W. Bandler, M.A. Ismail, J.E. Rayas-Sánchez and Q.J. Zhang

SOS-99-11-R

March 1999

© J.W. Bandler, M.A. Ismail, J.E. Rayas-Sánchez and Q.J. Zhang 1999

No part of this document may be copied, translated, transcribed or entered in any form into any machine without written permission. Address inquiries in this regard to Dr. J.W. Bandler. Excerpts may be quoted for scholarly purposes with full acknowledgment of source. This document may not be lent or circulated without this title page and its original cover.

NEUROMODELING OF MICROWAVE CIRCUITS EXPLOITING SPACE MAPPING TECHNOLOGY

John W. Bandler, *Fellow, IEEE*, Mostafa A. Ismail, *Student Member, IEEE*, José E. Rayas-Sánchez, *Senior Member, IEEE*, and Qi-Jun Zhang, *Senior Member, IEEE*

Abstract For the first time, we present modeling of microwave circuits using Artificial Neural Networks (ANN) based on Space Mapping (SM) technology. SM based neuromodels decrease the cost of training, improve generalization ability and reduce the complexity of the ANN topology with respect to the classical neuromodeling approach. Five creative, novel techniques are proposed to generate SM based neuromodels: Space Mapped Neuromodeling (SMN), Frequency-Dependent Space Mapped Neuromodeling (FDSMN), Frequency Space Mapped Neuromodeling (FSMN), Frequency Mapped Neuromodeling (FMN) and Frequency Partial-Space Mapped Neuromodeling (FPSM). A frequency-sensitive neuromapping is applied to overcome the limitations of empirical models developed under quasi-static conditions. Huber optimization is proposed to train the ANNs. We contrast SM based neuromodeling with the classical neuromodeling approach as well as with other state-of-the-art neuromodeling techniques. The SM based neuromodeling techniques are illustrated by two case studies: a microstrip right angle bend and a high-temperature superconducting (HTS) quarter-wave parallel coupled-line microstrip filter.

This work was supported in part by the Natural Sciences and Engineering Research Council of Canada under Grants OGP0007239 and STP0201832, and through the Micronet Network of Centres of Excellence. J.E. Rayas-Sánchez is funded by CONACYT (Consejo Nacional de Ciencia y Tecnología, Mexico), as well as by ITESO (Instituto Tecnológico y de Estudios Superiores de Occidente, Mexico).

J.W. Bandler, M.A. Ismail and J.E. Rayas-Sánchez are with the Simulation Optimization Systems Research Laboratory and the Department of Electrical and Computer Engineering, McMaster University, Hamilton, Ontario, Canada L8S 4K1.

J.W. Bandler is also with Bandler Corporation, P.O. Box 8083, Dundas, Ontario, Canada L9H 5E7.

Q.J. Zhang is with the Department of Electronics, Carleton University, 1125 Colonel By Drive, Ottawa, Canada K1S 5B6.

I. INTRODUCTION

A powerful new concept in neuromodeling of microwave circuits based on Space Mapping technology is presented. The ability of Artificial Neural Networks (ANN) to model high-dimensional and highly nonlinear problems is exploited in the implementation of the Space Mapping concept. By taking advantage of the vast set of empirical models already available, Space Mapping based neuromodels decrease the number of EM simulations for training, improve generalization ability and reduce the complexity of the ANN topology with respect to the classical neuromodeling approach.

Five innovative techniques are proposed to create Space Mapping based neuromodels for microwave circuits: Space Mapped Neuromodeling (SMN), Frequency-Dependent Space Mapped Neuromodeling (FDSMN), Frequency Space Mapped Neuromodeling (FSMN), Frequency Mapped Neuromodeling (FMN) and Frequency Partial-Space Mapped Neuromodeling (FPSM). Excepting SMN, all these approaches establish a frequency-sensitive neuromapping to expand the frequency region of accuracy of the empirical models already available for microwave components that were developed using quasi-static analysis. We contrast our approach with the classical neuromodeling approach as well as with other state-of-the-art neuromodeling techniques.

For the first time [1], Huber optimization is proposed to efficiently train the ANNs as a powerful alternative to the popular backpropagation algorithm. The Space Mapping based neuromodeling techniques are illustrated by two case studies: a microstrip right angle bend and a high-temperature superconducting (HTS) quarter-wave parallel coupled-line microstrip filter.

II. SPACE MAPPING CONCEPT

Space Mapping (SM) is a novel concept for circuit design and optimization that combines the computational efficiency of coarse models with the accuracy of fine models. The coarse models are typically empirical equivalent circuit engineering models, which are computationally very efficient but often have a limited validity range for their parameters, beyond which the simulation results may become inaccurate. On the other hand, detailed or “fine” models can be provided by an electromagnetic (EM)

simulator, or even by direct measurements: they are very accurate but CPU intensive. The SM technique establishes a mathematical link between the coarse and the fine models, and directs the bulk of CPU intensive evaluations to the coarse model, while preserving the accuracy and confidence offered by the fine model. The SM technique was originally developed by Bandler *et al.* [2].

Let the vectors \mathbf{x}_c and \mathbf{x}_f represent the design parameters of the coarse and fine models, respectively, and $\mathbf{R}_c(\mathbf{x}_c)$ and $\mathbf{R}_f(\mathbf{x}_f)$ the corresponding model responses. \mathbf{R}_c is much faster to calculate but less accurate than \mathbf{R}_f .

As illustrated in Fig. 1, the aim of SM optimization is to find an appropriate mapping \mathbf{P} from the fine model parameter space \mathbf{x}_f to the coarse model parameter space \mathbf{x}_c

$$\mathbf{x}_c = \mathbf{P}(\mathbf{x}_f) \quad (1)$$

such that

$$\mathbf{R}_c(\mathbf{P}(\mathbf{x}_f)) \approx \mathbf{R}_f(\mathbf{x}_f) \quad (2)$$

Once the mapping is found, the coarse model can be used for fast and accurate simulations.

III. NEUROMODELING MICROWAVE CIRCUITS

The ability to learn and generalize from data, the non-linear processing nature, and the massively parallel structure make the ANN particularly suitable in modeling high-dimensional and highly nonlinear problems, as in the case of microwave circuits.

The size of an ANN model does not grow exponentially with dimension and, in theory, can approximate any degree of nonlinearity to any desired level of accuracy, provided a deterministic relationship between input and target exists [3]. The most widely used ANN paradigm in the microwave arena [1] is the multi-layer perceptron (MLP), which is usually trained by the well established backpropagation algorithm.

ANN models are computationally more efficient than EM or physics-based models and can be more accurate than empirical models. It has been demonstrated [4, 5] that ANNs are suitable models for

microwave circuit yield optimization and statistical design.

For microwave problems the learning data is usually obtained by either EM simulation or by measurement. Large amounts of learning data are typically needed to ensure model accuracy. This is very expensive since the simulation/measurements must be performed for many combinations of different values of geometrical, material, process and input signal parameters. This is the principal drawback of classical ANN modeling. Without sufficient learning samples, the neural models may not be reliable.

A popular alternative to reduce the dimension of the learning set is to carefully select the learning points using the Design of Experiments (DoE) methodology. Another way to speed up the learning process is proposed in [1] by means of preliminary neural clusterization of similar responses using the Self Organizing Feature Map (SOM) approach.

Innovative strategies have been proposed to reduce the learning data needed and to improve the generalization capabilities of an ANN by incorporating empirical models: the hybrid EM-ANN modeling approach, the PKI modeling method, and the knowledge based ANN (KBNN) approach.

In the hybrid EM-ANN modeling approach [6], the difference in S -parameters between the available coarse model and the fine model is used to train the corresponding ANN, as illustrated in Fig. 2, reducing the number of fine model simulations due to a simpler input-output relationship.

For the PKI method [6], the coarse model output is used as input for the ANN in addition to the other inputs (physical parameters and frequency). The ANN is trained such that its response is approximately equal to the fine model response, as illustrated in Fig. 3. The PKI approach has shown better accuracy than the EM-ANN approach, but it requires a more complex ANN.

In the knowledge based ANN approach [7] (KBNN) the microwave empirical or semi-analytical information is incorporated into the internal structure of the ANN, as illustrated in Fig. 4. Knowledge Based ANNs are non fully connected networks, with a layer assigned to the microwave knowledge in the form of single or multidimensional functions. Since these empirical functions are used for some neurons instead of standard activation functions, KBNNs do not follow a regular multilayer perceptron and are trained using other methods than the conventional backpropagation.

IV. SPACE MAPPING BASED NEUROMODELING

We propose innovative schemes to combine SM technology and ANN for the modeling of high frequency components. The fundamental idea is to construct a nonlinear multidimensional vector mapping function \mathbf{P} from the fine to the coarse input space using an ANN. This can be done in a variety of ways, to make a better use of the coarse model information for developing the neuromodel. The implicit knowledge in the coarse model that can be considered as an “expert”, not only allows us to decrease the number of learning points needed, but also to reduce the complexity of the ANN and to improve the generalization performance.

In the Space Mapped Neuromodeling (SMN) approach the mapping from the fine to the coarse parameter space is implemented by an ANN. Fig. 5 illustrates the SMN concept. We have to find the optimal set of the internal parameters of the ANN, such that the coarse model response is as close as possible to the fine model response for all the learning points.

The mapping can be found by solving the optimization problem

$$\min_{\mathbf{w}} \left\| [\mathbf{e}_1^T \quad \mathbf{e}_2^T \quad \cdots \quad \mathbf{e}_l^T]^T \right\| \quad (3)$$

where vector \mathbf{w} contains the internal parameters of the neural network (weights, bias, etc.) selected as optimization variables, l is the total number of learning samples, and \mathbf{e}_k is the error vector given by

$$\mathbf{e}_k = \mathbf{R}_f(\mathbf{x}_{f_i}, freq_j) - \mathbf{R}_c(\mathbf{x}_c, freq_j) \quad (4a)$$

$$\mathbf{x}_c = \mathbf{P}(\mathbf{x}_{f_i}) \quad (4b)$$

with

$$i = 1, \dots, B_p \quad (5a)$$

$$j = 1, \dots, F_p \quad (5b)$$

$$k = j + F_p(i-1) \quad (5c)$$

where B_p is the number of training base points for the input design parameters and F_p is the number of frequency points per frequency sweep. It is seen that the total number of learning samples is $l = B_p F_p$.

The specific characteristics of \mathbf{P} depend on the ANN paradigm chosen whose internal parameters are in \mathbf{w} .

Once the mapping is found, i.e., once the ANN is trained, a space mapped neuromodel for fast, accurate evaluations is immediately available.

Including Frequency in the Neuromapping

Many of the empirical models already available for microwave circuits were developed using methods for quasi-static analysis. For instance, in the case of microstrip circuits, it is often assumed that the mode of wave propagation in the microstrip is pure TEM [8]. This implies that the effective dielectric constant ϵ_e and the characteristic impedance Z_o don't vary with frequency. Nevertheless, non-TEM behavior causes ϵ_e and Z_o to be functions of frequency. Therefore, these empirical models usually yield good accuracy over a limited range of low frequencies.

A method to directly overcome this limitation is by establishing a frequency-sensitive mapping from the fine to the coarse input spaces. This is realized by considering frequency as an extra input variable of the ANN that implements the mapping.

In the Frequency-Dependent Space Mapped Neuromodeling (FDSMN) approach, illustrated in Fig. 6, both coarse and fine models are simulated at the same frequency, but the mapping from the fine to the coarse parameter space is dependent on the frequency. The mapping is found by solving the same optimization problem stated in (3) but substituting (4) by

$$\mathbf{e}_k = \mathbf{R}_f(\mathbf{x}_{f_i}, freq_j) - \mathbf{R}_c(\mathbf{x}_c, freq_j) \quad (6a)$$

$$\mathbf{x}_c = \mathbf{P}(\mathbf{x}_{f_i}, freq_j) \quad (6b)$$

With a more comprehensive domain, the Frequency Space Mapped Neuromodeling (FSMN) technique establishes a mapping not only for the design parameters but also for the frequency variable, such that the coarse model is simulated at a mapped frequency f_c to match the fine model response. This is realized by adding an extra output to the ANN that implements the mapping, as shown in Fig. 7. The mapping is found by solving the same optimization problem stated in (3) but interchanging (4) by

$$\mathbf{e}_k = \mathbf{R}_f(\mathbf{x}_{f_i}, freq_j) - \mathbf{R}_c(\mathbf{x}_c, f_c) \quad (7a)$$

$$\begin{bmatrix} \mathbf{x}_c \\ f_c \end{bmatrix} = \mathbf{P}(\mathbf{x}_{f_i}, freq_j) \quad (7b)$$

It is not uncommon to find microwave problems where the coarse model behaves almost as the fine model does but with a shifted frequency response, i.e., the shapes of the responses are nearly identical but shifted. For those cases, a good alignment between both responses is achieved by simulating the coarse model at a different frequency. Frequency Mapped Neuromodeling technique implements this strategy, as shown in Fig. 8, by simulating the coarse model with the same physical parameters used by the fine model, but a mapped frequency f_c to align both responses. The mapping is found by solving the same optimization problem stated in (3) but replacing (4) by

$$\mathbf{e}_k = \mathbf{R}_f(\mathbf{x}_{f_i}, freq_j) - \mathbf{R}_c(\mathbf{x}_{f_i}, f_c) \quad (8a)$$

$$f_c = P(\mathbf{x}_{f_i}, freq_j) \quad (8b)$$

Mapping the whole set of physical parameters, as in the SMN, FDSMN and FSMN techniques, might lead to singularities in the coarse model response during training. This problem is overcome by establishing a partial mapping for the physical parameters, making even more efficient use of the implicit knowledge in the coarse model. Mapping only some of the physical parameters can be enough to obtain acceptable accuracy in the neuromodel for many microwave problems. This allows us a significant reduction in the ANN complexity w.r.t. the SMN, FDSMN and FSMN techniques and a significant reduction in the training time, because less optimization variables are used. Frequency Partial-Space Mapped Neuromodeling (FPSMN) is illustrated in Fig. 9. The mapping for this technique is found by solving the same optimization problem stated in (3) but replacing (4) by

$$\mathbf{e}_k = \mathbf{R}_f(\mathbf{x}_{f_i}, freq_j) - \mathbf{R}_c(\mathbf{x}_{f_i}^s, \mathbf{x}_c^s, f_c) \quad (9a)$$

$$\begin{bmatrix} \mathbf{x}_c^s \\ f_c \end{bmatrix} = \mathbf{P}(\mathbf{x}_{f_i}, freq_j) \quad (9b)$$

where $\mathbf{x}_{f_i}^s$ vector contains a suitable subset of the design physical parameters \mathbf{x}_{f_i} at the i th training base point.

Finally, there can be microwave problems where the complete set of responses contained in \mathbf{R}_f is difficult to approximate using the coarse model with a single ANN. In those cases, the learning task can be distributed among a number of ANNs, which in turn divides the output space into a set of subspaces. The corresponding ANNs can then be trained individually, to match each response (or subset of responses) contained in \mathbf{R}_f . This implies the solution of several independent optimization problems instead of a single one.

Starting Point and Learning Data Samples

The starting point for the optimization problem stated in (3) is the initial set of internal parameters of the ANN, $\mathbf{w}^{(1)}$, that is chosen assuming that the coarse model is actually a good model and therefore the mapping is not necessary. In other words, $\mathbf{w}^{(1)}$ is chosen such that the ANN implements a unit mapping \mathbf{P} ($\mathbf{x}_c = \mathbf{x}_f$ and/or $f_c = freq$). This is applicable to the five proposed SM based neuromodeling techniques.

The ANN must be trained to learn the mapping between the coarse and the fine input spaces within the region of interest. In order to keep a reduced set of learning data samples, an n -dimensional star distribution for the base learning points is considered in this work, as in [9] (see Fig. 10). It is seen that the number of learning base points for a microwave circuit with n design parameters is $B_p = 2n + 1$.

Since we want to maintain a minimum number of learning points (or fine evaluations), the complexity of the ANN is critical. It is well known that too small an ANN cannot approximate the desired input-output relationship, while ANNs with too many internal parameters perform correctly on the learning set, but give poor generalization ability. We have to use the simplest ANN that gives adequate training error and acceptable generalization performance.

Mapping with a Three Layer Perceptron

A possible scheme to implement the mapping using a three-layer perceptron with h hidden

neurons, for both the SMN approach as well as the FDSMN approach, is illustrated in Fig. 11. Here, the total number of optimization variables for (3) is $2h(n+1)+n$, where n is the number of physical parameters to be mapped and h is the number of hidden neurons. The adaptation of this paradigm to all the other three cases is realized by considering an additional output for the mapped frequency f_c and disabling the corresponding inputs and/or outputs.

In this work we considered sigmoid functions as well as hyperbolic tangent functions to implement the nonlinear activation functions for the neurons in the hidden layer.

V. CASE STUDIES

A Microstrip Right Angle Bend

Consider a microstrip right angle bend, as illustrated in Fig. 12, with the following input parameters: conductor width W , substrate height H , substrate dielectric constant ϵ_r , and operating frequency $freq$. Three neuromodels exploiting SM technology are developed for the region of interest shown in Table I.

Gupta's model [8], consisting of a lumped LC circuit whose parameter values are given by analytical functions of the physical quantities W , H and ϵ_r , is taken as the "coarse" model and implemented in OSA90/hopeTM [10]. Sonnet's *em*TM [11] is used as the fine model. To parameterize the structure, the Geometry Capture [12] technique available in EmpipeTM [13] is utilized.

Fig. 13 shows typical responses of the coarse and fine models before any neuromodeling, using a frequency step of 2 GHz ($F_p = 21$). The coarse and fine models are compared in Fig. 14 using 50 random test base-points with uniform statistical distribution within the region of interest (1050 test samples). Gupta's model, in this region of physical parameters, yields acceptable results for frequencies less than 10 GHz.

With a star distribution for the learning base points ($n = 3$, $B_p = 7$), 147 learning samples ($l = 147$) are used for three SM based neuromodels, and the corresponding ANNs were implemented and trained

within OSA90/hope™. Huber optimization was employed as the training algorithm, exploiting its robust characteristics for data fitting [14].

Fig. 15 shows the results for the SMN model implemented with a three layer perceptron with 3 input neurons, 6 hidden neurons, and 3 output neurons (3LP:3-6-3). A FDSMN model is developed using a 3LP:4-7-3, and the improved results are shown in Fig. 16. In Fig. 17 the results for the FSMN model with a 3LP:4-8-4 are shown, that are even better (as expected). To implement the FSMN approach, an OSA90 child program is employed to simulate the coarse model with a different frequency variable using Datapipe. It is seen that the FSMN model yields excellent results for the whole frequency range of interest, overcoming the frequency limitations of the empirical model by a factor of four.

To compare these results with those from a classical neuromodeling approach, an ANN was developed using *NeuroModeler* [15]. Training the ANN with the same 147 learning samples, the best results were obtained for a 3LP:4-15-4 trained with the conjugate gradient and quasi-Newton methods. Due to the small number of learning samples, this approach did not provide good generalization capabilities, as illustrated in Fig. 18. To produce similar results to those in Fig. 17 using the same ANN complexity, the learning samples have to increase from 147 to 315.

Fig. 19 summarizes the different neuromodeling approaches applied to this case study.

HTS Quarter-Wave Parallel Coupled-Line Microstrip Filter

Fig. 20 illustrates a high-temperature superconducting (HTS) quarter-wave parallel coupled-line microstrip filter to be modeled in the region of interest shown in Table II. L_1 , L_2 and L_3 are the lengths of the parallel coupled-line sections and S_1 , S_2 and S_3 are the gaps between the sections. The width W is the same for all the sections as well as for the input and output microstrip lines, of length L_0 . A lanthanum aluminate substrate with thickness H and dielectric constant ϵ is used. The metalization is considered lossless. Two SM based neuromodels are developed in the region of interest, taking as design parameters $\mathbf{x}_f = [L_1 L_2 L_3 S_1 S_2 S_3]^T$.

It has been already shown [16] that the responses of this narrow bandwidth filter are very

sensitive to dimensional changes. Sonnet's *em*TM driven by EmpipeTM was employed as the fine model, using a high-resolution grid with a 1mil×1mil cell size.

Sections of OSA90/hopeTM built-in linear elements MSL (microstrip line) and MSCL (two-conductor symmetrical coupled microstrip lines) connected by circuit theory over the same MSUB (microstrip substrate definition) are taken as the “coarse” model.

Typical responses of the coarse and fine models before any neuromodeling are shown in Fig. 21, using a frequency step of 0.02 GHz ($F_p = 14$). About 10 hrs of CPU simulation time was needed for a single frequency sweep on an HP C200-RISC workstation. Following a multidimensional star distribution ($n = 6$), 13 learning base points are used ($l = 182$). To evaluate the generalization performance, 7 testing base points not seen in the learning set are used.

The coarse and fine models before neuromodeling are compared in Fig. 22, at both the learning and the testing sets, showing very large errors in the coarse model with respect *em*TM due to a shifting in its frequency response, as seen in Fig. 21.

To explore the effects of simulating the coarse model at a mapped frequency, a FMN model (see Fig. 8) implemented with a 3LP:7-5-1 is developed using Huber optimization. The FMN approach yields good frequency alignment between both responses, as shown in Fig. 23. The corresponding training and generalization errors are shown in Fig. 24.

Excellent results are obtained for the FPSMN modeling approach (see Fig. 9), taking $\mathbf{x}_c^s = [L_{1c} S_{1c}]^T$ and $\mathbf{x}_f^s = [L_2 L_3 S_2 S_3]^T$ and using a 3LP:7-7-3 trained with Huber optimization. As illustrated in Fig. 25, an outstanding agreement between the fine model and the FPSMN model is achieved. The learning and generalization performance is shown in Fig. 26.

As a final test, both the FPSMN model and the fine model are simulated at three different base points using a very fine frequency sweep, with a frequency step of 0.005GHz. Remarkable matching is obtained, as illustrated in Fig. 27.

VI. CONCLUSIONS

We present novel applications of Space Mapping technology to the neuromodeling of microwave circuits. Five powerful techniques to generate SM based neuromodels are described and illustrated: Space Mapped Neuromodeling (SMN), Frequency-Dependent Space Mapped Neuromodeling (FDSMN), Frequency Space Mapped Neuromodeling (FSMN), Frequency Mapped Neuromodeling (FMN) and Frequency Partial-Space Mapped Neuromodeling (FPSMN). These techniques exploit the vast set of empirical models already available, decrease the number of fine model evaluations needed for training, improve generalization ability and reduce the complexity of the ANN topology w.r.t. the classical neuromodeling approach. Frequency-sensitive neuromapping is demonstrated to be a clever strategy to expand the usefulness of empirical models that were developed using quasi-static analysis. FMN is presented as an effective method to align frequency-shifted responses. By establishing a partial mapping for the physical parameters, a more efficient use of the implicit knowledge in the coarse model is achieved and singularities in the coarse model response during training can be avoided. As an original alternative to the classical backpropagation algorithm, Huber optimization is employed to efficiently train the neuromapping, exploiting its robust characteristics for data fitting.

ACKNOWLEDGEMENT

The authors thank Dr. J.C. Rautio, President, Sonnet Software, Inc., Liverpool, NY, for making *em*TM available.

REFERENCES

- [1] P. Burrascano and M. Mongiardo, "A review of artificial neural networks applications in microwave CAD," *Int. J. RF and Microwave CAE*, Special Issue on Applications of ANN to RF and Microwave Design, vol. 9, 1999.
- [2] J.W. Bandler, R.M. Biernacki, S.H. Chen, P.A. Grobelny and R.H. Hemmers, "Space mapping technique for electromagnetic optimization," *IEEE Trans. Microwave Theory Tech.*, vol. 42, 1994, pp. 2536-2544.
- [3] H. White, A.R. Gallant, K. Hornik, M. Stinchcombe and J. Wooldrige, *Artificial Neural*

Networks: Approximation and Learning Theory. Oxford, UK: Blackwell, 1992.

- [4] A.H. Zaabab, Q.J. Zhang and M.S. Nakhla, "A neural network modeling approach to circuit optimization and statistical design," *IEEE Trans. Microwave Theory Tech.*, vol. 43, 1995, pp. 1349-1358.
- [5] P. Burrascano, M. Dionigi, C. Fancelli and M. Mongiardo, "A neural network model for CAD and optimization of microwave filters," *IEEE MTT-S Int. Microwave Symp. Dig.* (Baltimore, MD), 1998, pp. 13-16.
- [6] P. Watson and K.C. Gupta, "EM-ANN models for microstrip vias and interconnects in multilayer circuits," *IEEE Trans. Microwave Theory Tech.*, vol. 44, 1996, pp. 2495-2503.
- [7] F. Wang and Q.J. Zhang, "Knowledge based neuromodels for microwave design," *IEEE Trans. Microwave Theory Tech.*, vol. 45, 1997, pp. 2333-2343.
- [8] K.C. Gupta, R. Garg, I.J. Bahl, *Microstrip Lines and Slotlines*. Dedham, MA: Artech House, 1979.
- [9] R.M. Biernacki, J.W. Bandler, J. Song and Q.J. Zhang, "Efficient quadratic approximation for statistical design," *IEEE Trans. Circuit Syst.*, vol. 36, 1989, pp. 1449-1454.
- [10] OSA90/hope™ Version 4.0, formerly Optimization Systems Associates Inc., P.O. Box 8083, Dundas, Ontario, Canada L9H 5E7, 1997, now HP EEsof Division, Hewlett-Packard Company, 1400 Fountaingrove Parkway, Santa Rosa, CA 95403-1799.
- [11] *em*™ Version 4.0b, Sonnet Software, Inc., 1020 Seventh North Street, Suite 210, Liverpool, NY 13088, 1997.
- [12] J.W. Bandler, R.M. Biernacki and S.H. Chen, "Parameterization of arbitrary geometrical structures for automated electromagnetic optimization," *IEEE MTT-S Int. Microwave Symp. Dig.* (San Francisco, CA), 1996, pp. 1059-1062.
- [13] Empipe™ Version 4.0, formerly Optimization Systems Associates Inc., P.O. Box 8083, Dundas, Ontario, Canada L9H 5E7, 1997, now HP EEsof Division, Hewlett-Packard Company, 1400 Fountaingrove Parkway Santa Rosa, CA 95403-1799.
- [14] J.W. Bandler, S.H. Chen, R.M. Biernacki, L. Gao, K. Madsen and H. Yu, "Huber optimization of circuits: a robust approach," *IEEE Trans. Microwave Theory Tech.*, vol. 41, 1993, pp. 2279-2287.
- [15] *NeuroModeler* Version 1.0, Prof. Q.J. Zhang, Dept. of Electronics, Carleton University, 1125 Colonel By Drive, Ottawa, Ontario, Canada, K1S 5B6, 1998.
- [16] J.W. Bandler, R.M. Biernacki, S.H. Chen, W.J. Getsinger, P.A. Grobelny, C. Moskowitz and S.H. Talisa, "Electromagnetic design of high-temperature superconducting microwave filters," *Int. J. Microwave and Millimeter-Wave CAE*, vol. 5, 1995, pp. 331-343.

TABLE I
REGION OF INTEREST FOR THE
MICROSTRIP RIGHT ANGLE BEND

Parameter	Minimum value	Maximum value
W	20 mil	30 mil
H	8 mil	16 mil
ϵ_r	8	10
$freq$	1 GHz	41 GHz

TABLE II
REGION OF INTEREST FOR THE HTS FILTER

Parameter	Minimum value	Maximum value
W	7 mil	7 mil
H	20 mil	20 mil
ϵ_r	23.425	23.425
loss tang	3×10^{-5}	3×10^{-5}
L_0	50 mil	50 mil
L_1	175 mil	185 mil
L_2	190 mil	210 mil
L_3	175 mil	185 mil
S_1	18 mil	22 mil
S_2	75 mil	85 mil
S_3	70 mil	90 mil
$freq$	3.901 GHz	4.161 GHz

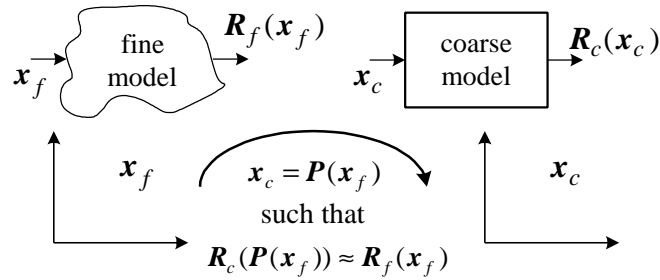


Fig. 1. Illustration of the aim of Space Mapping (SM).

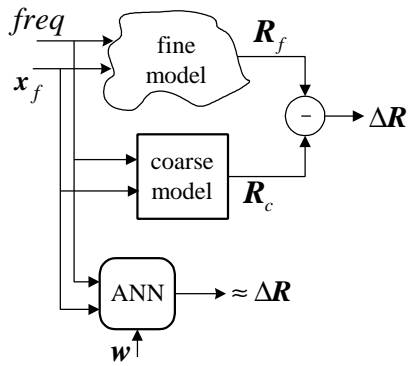


Fig. 2. EM-ANN neuromodeling concept [6].

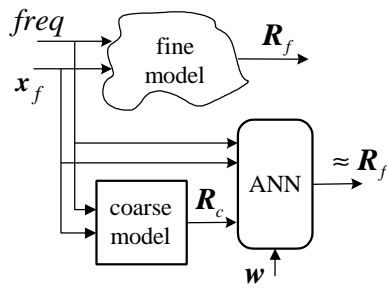


Fig. 3. PKI neuromodeling concept [6].

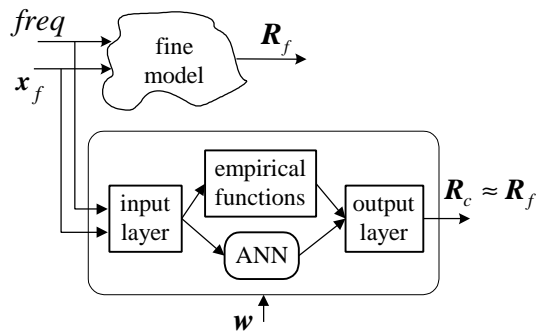


Fig. 4. KBNN neuromodeling concept [7].

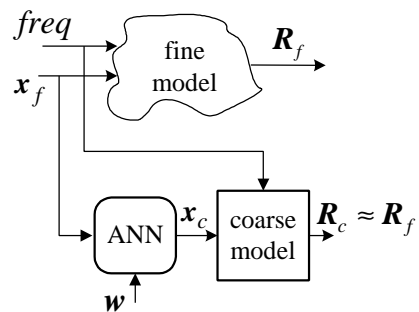


Fig. 5. Space Mapped Neuromodeling (SMN) concept.

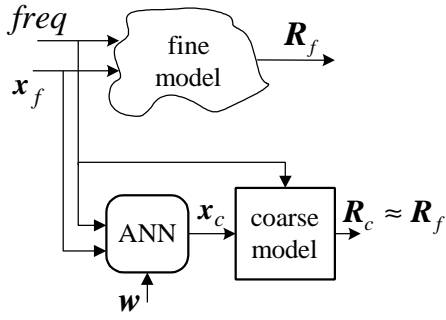


Fig. 6. Frequency-Dependent Space Mapped Neuromodeling (FDSMN).

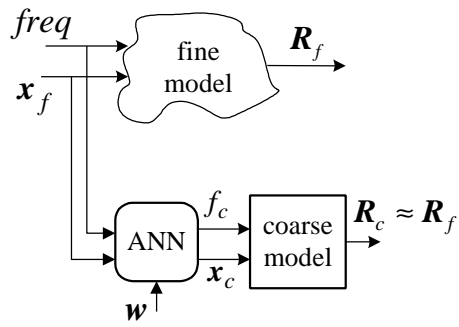


Fig. 7. Frequency Space Mapped Neuromodeling (FSMN).

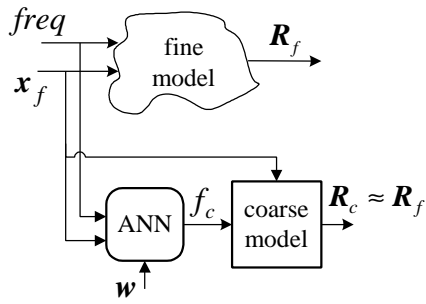


Fig. 8. Frequency Mapped Neuromodeling (FMN).

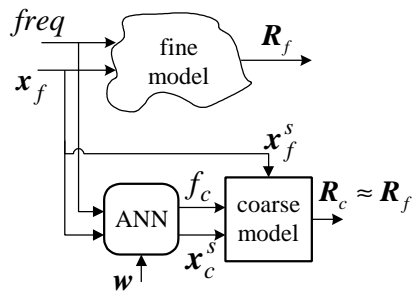


Fig. 9. Frequency Partial-Space Mapped Neuromodeling (FPSMN).

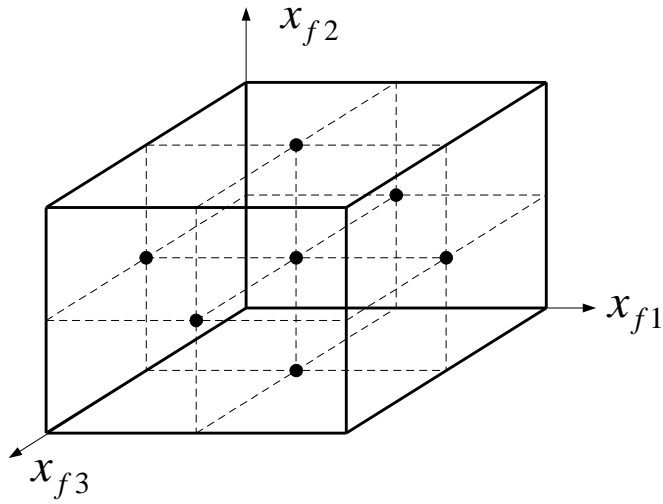


Fig. 10. Three-dimensional star distribution for the learning base points.

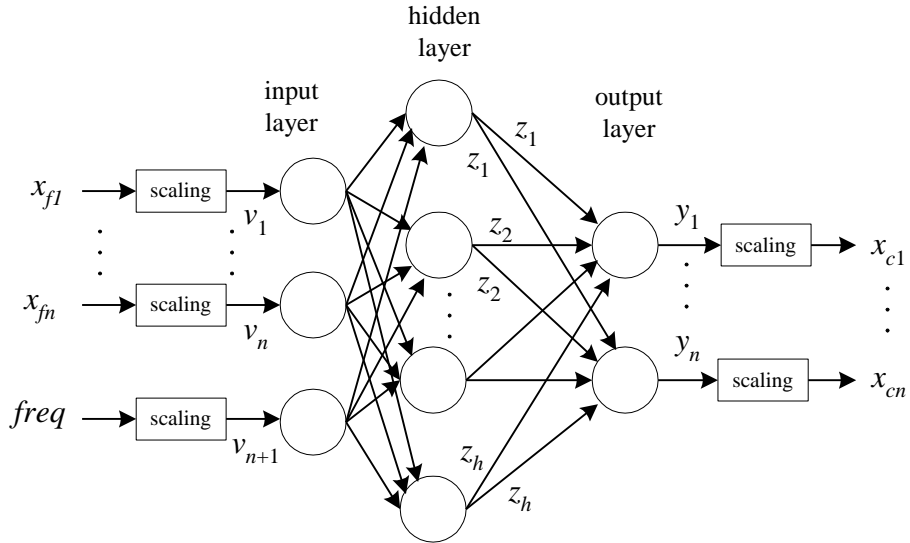


Fig. 11. Implementing the frequency-dependent neuromapping with a three-layer perceptron as in Fig. 6.

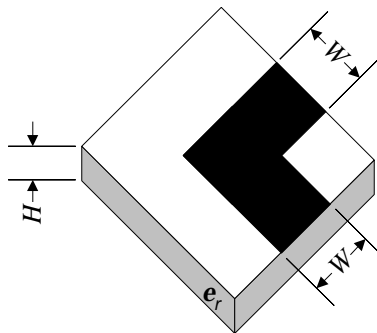
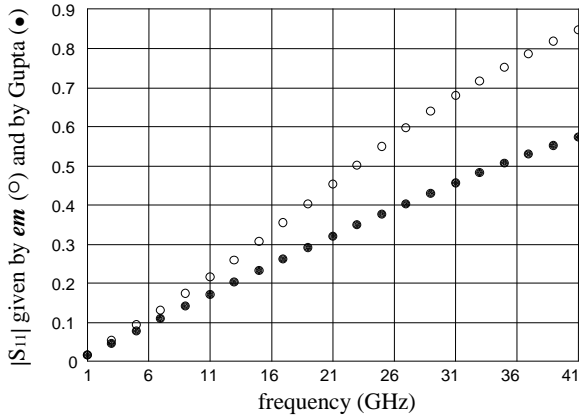
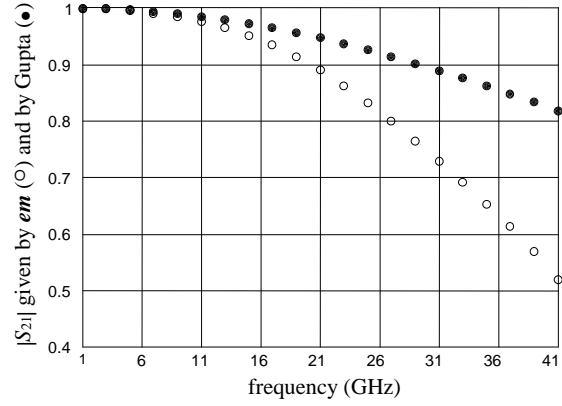


Fig. 12. Microstrip right angle bend.

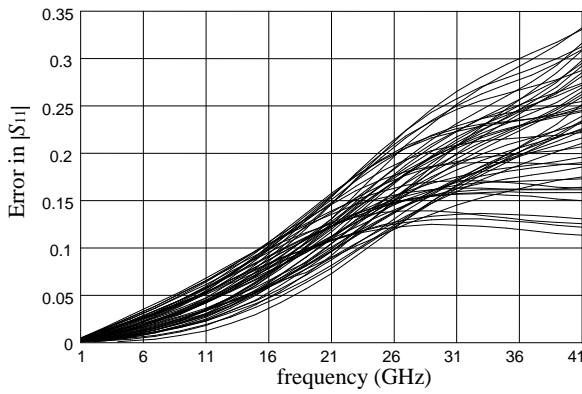


(a)

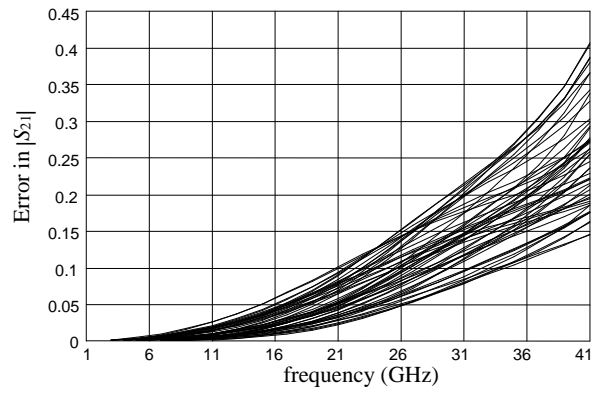


(b)

Fig. 13. Typical responses of the right angle bend using em^{TM} (o) and Gupta model (•) before any neuromodeling: (a) $|S_{11}|$, (b) $|S_{21}|$.

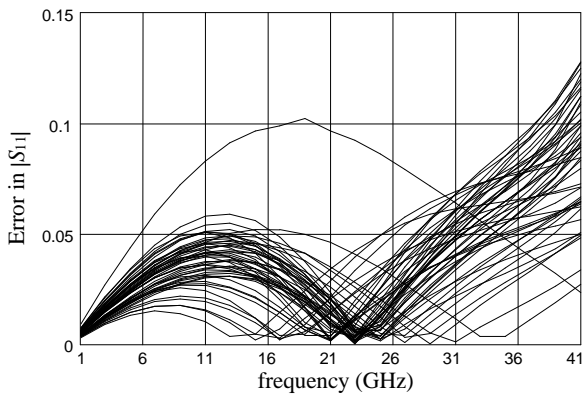


(a)

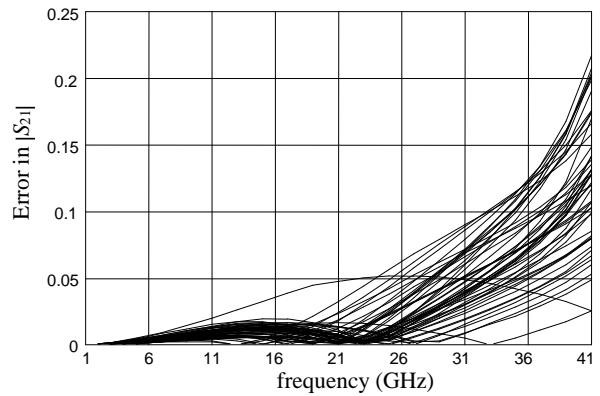


(b)

Fig. 14. Comparison between em^{TM} and Gupta model of a right angle bend: (a) error in $|S_{11}|$ with respect to em^{TM} , (b) error in $|S_{21}|$ with respect to em^{TM} .

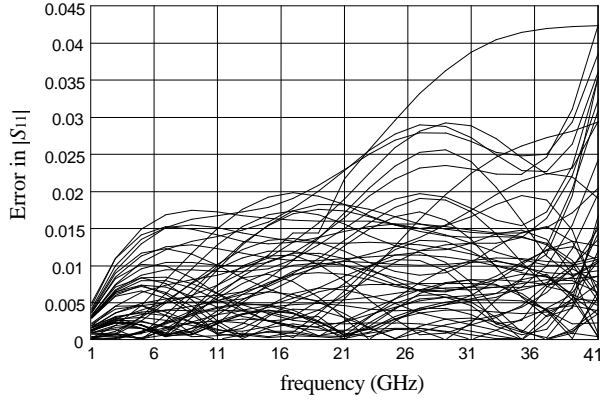


(a)

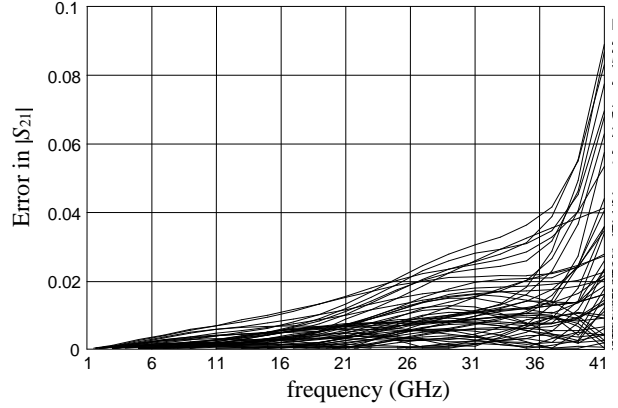


(b)

Fig. 15. Comparison between em^{TM} and SMN model of a right angle bend: (a) error in $|S_{11}|$ with respect to em^{TM} , (b) error in $|S_{21}|$ with respect to em^{TM} .

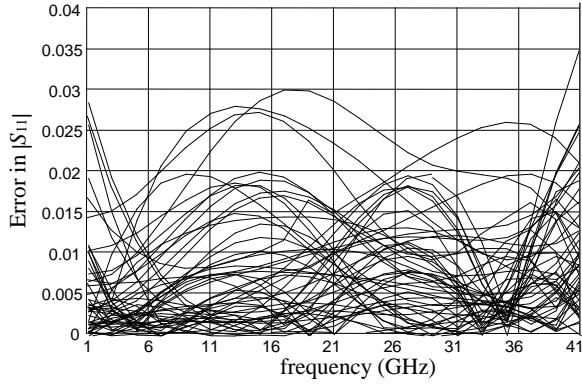


(a)

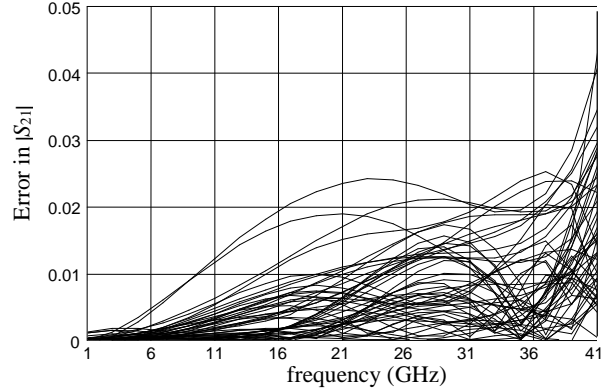


(b)

Fig. 16. Comparison between em^{TM} and FDSMN model of a right angle bend:
 (a) error in $|S_{11}|$ with respect to em^{TM} , (b) error in $|S_{21}|$ with respect to em^{TM} .

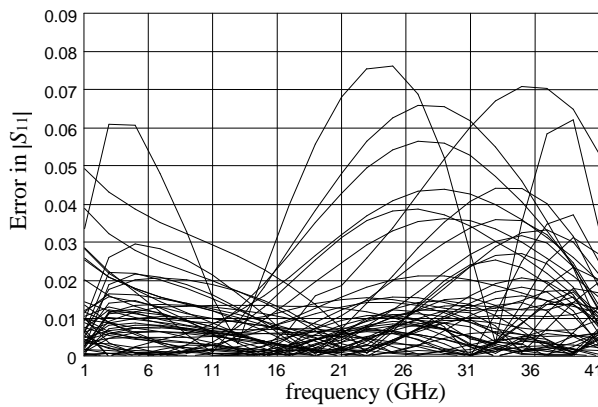


(a)

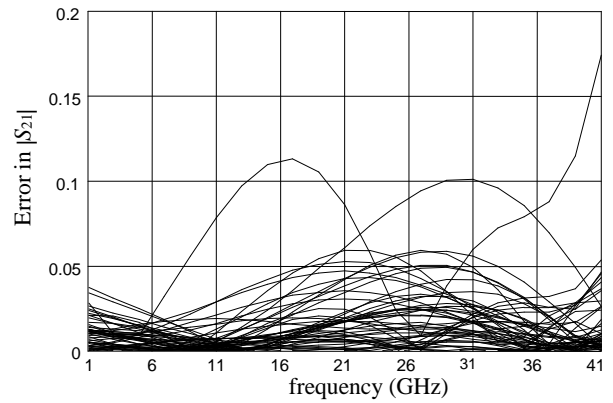


(b)

Fig. 17. Comparison between em^{TM} and FSMN model of a right angle bend:
 (a) error in $|S_{11}|$ with respect to em^{TM} , (b) error in $|S_{21}|$ with respect to em^{TM} .



(a)



(b)

Fig. 18. Comparison between em^{TM} and classical neuromodel of a right angle bend:
 (a) error in $|S_{11}|$ with respect to em^{TM} , (b) error in $|S_{21}|$ with respect to em^{TM} .

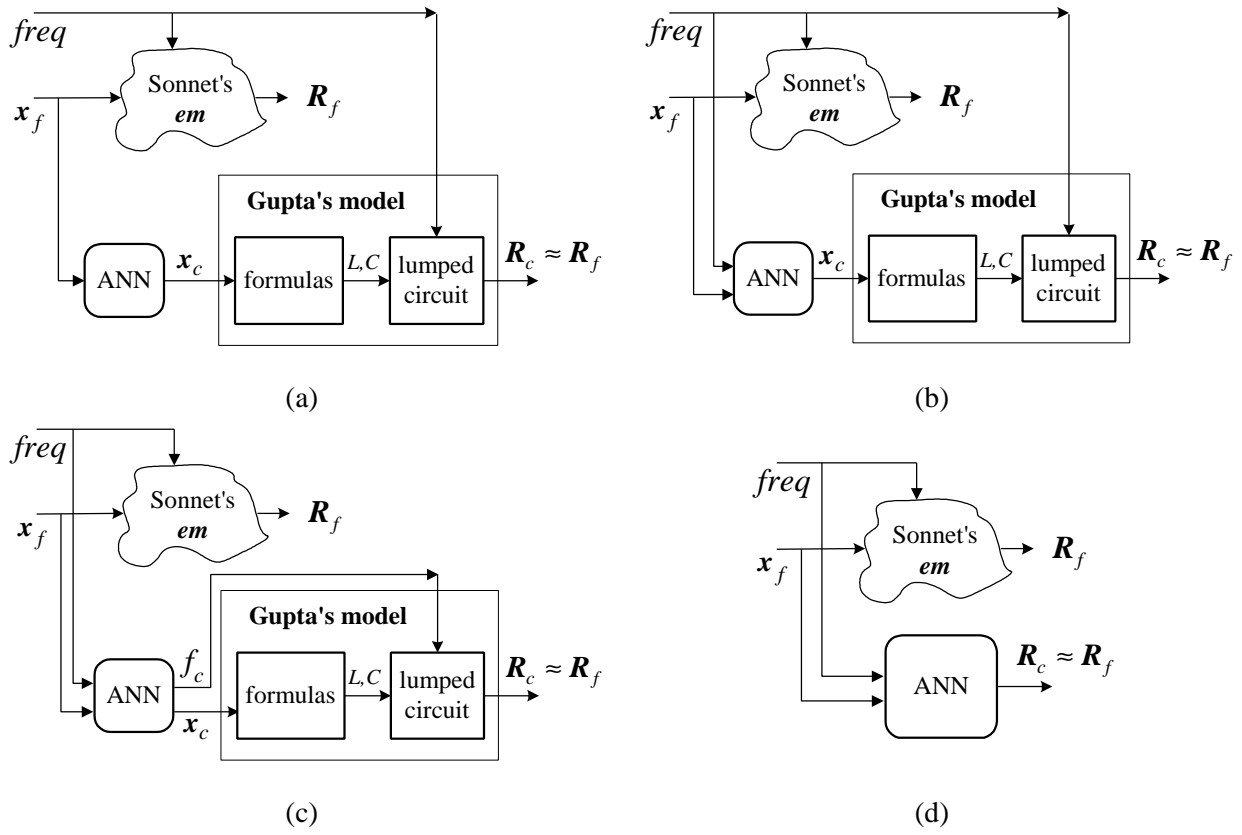


Fig. 19. Different neuromodeling approaches for the right angle bend:
 (a) SMN, (b) FDSMN, (c) FSMN, and (d) classical neuromodeling.

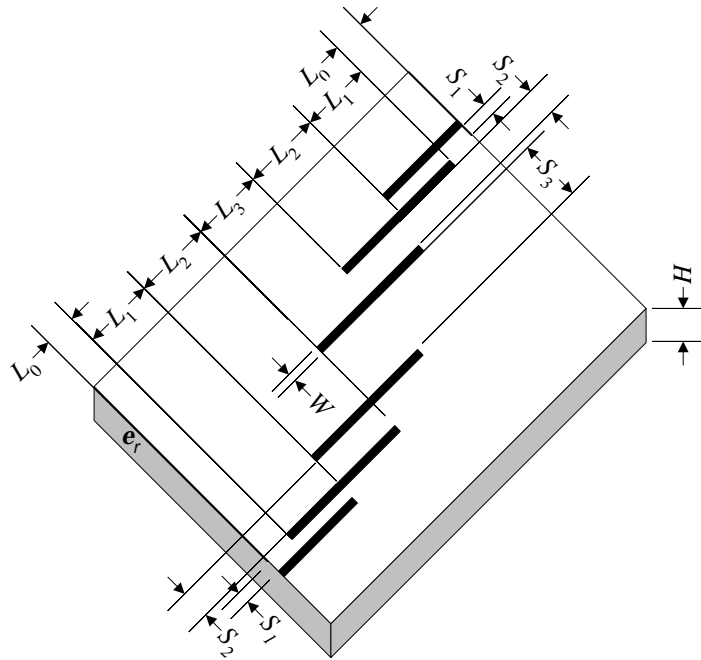


Fig. 20. HTS quarter-wave parallel coupled-line microstrip filter.

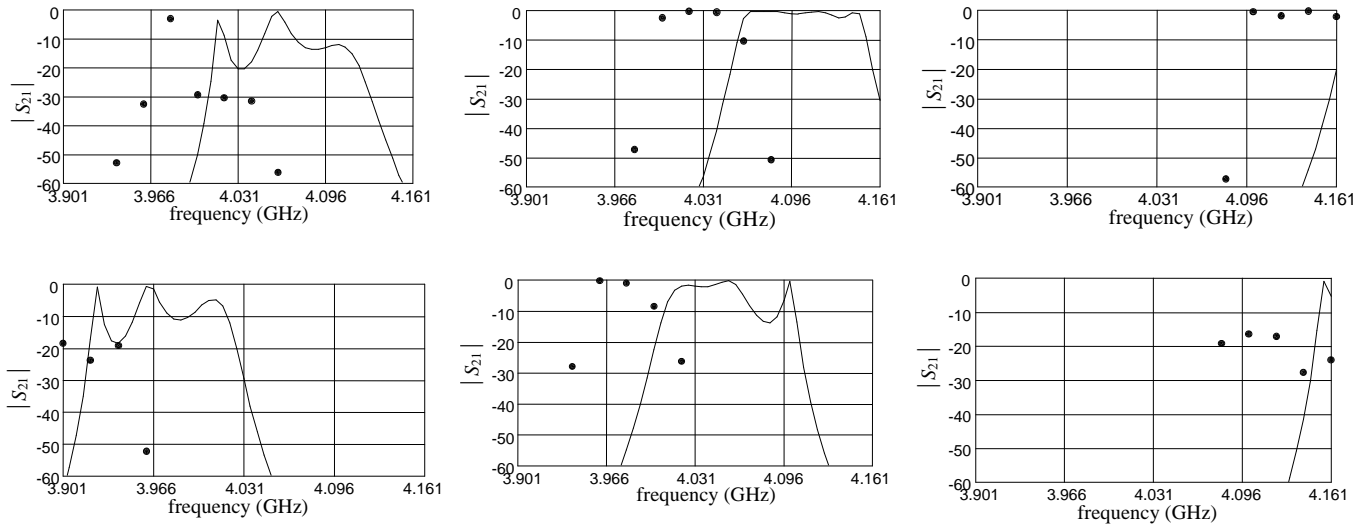


Fig. 21. Typical responses of the HTS filter using em^{TM} (●) and OSA90/hope TM model (–) before any neuromodeling at three learning and three testing points.

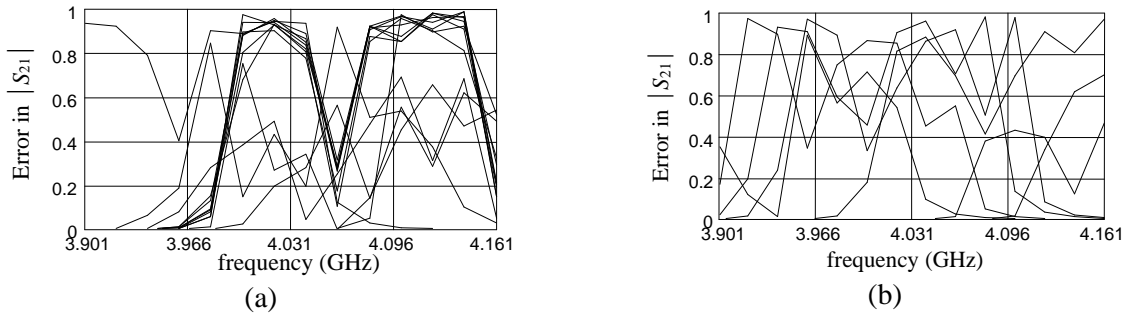


Fig. 22. Coarse model error w.r.t. em^{TM} before any neuromodeling: (a) in the learning set, (b) in the testing set.

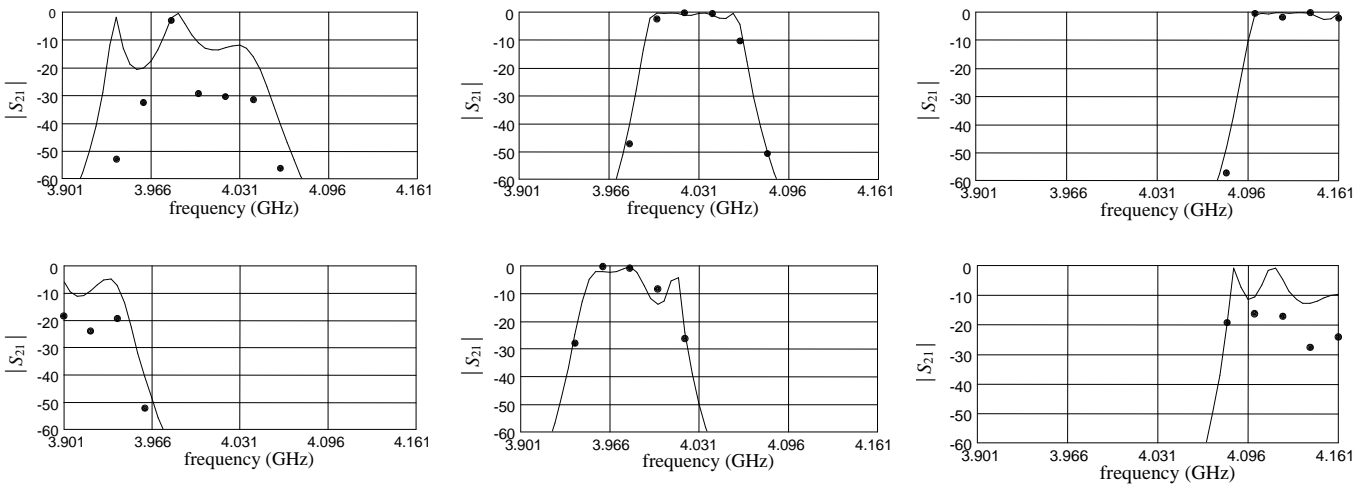
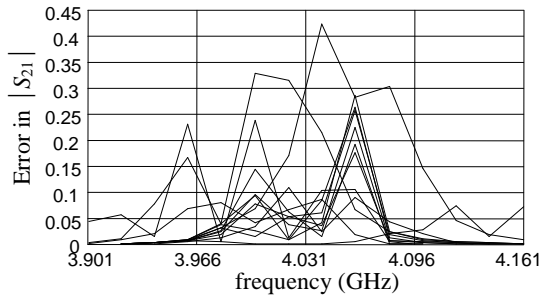
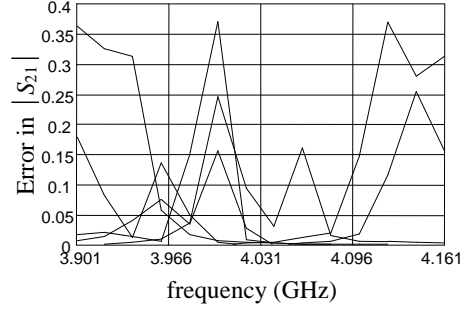


Fig. 23. Typical responses of the HTS filter using em^{TM} (●) and FMN model (–) at the same three learning and three testing points as in Fig. 21.



(a)



(b)

Fig. 24. FMN model error w.r.t. em^{TM} : (a) in the learning set, (b) in the testing set.

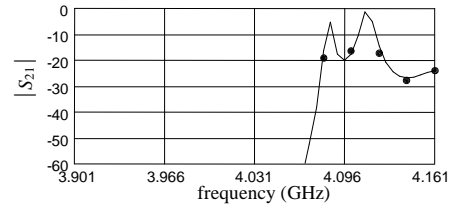
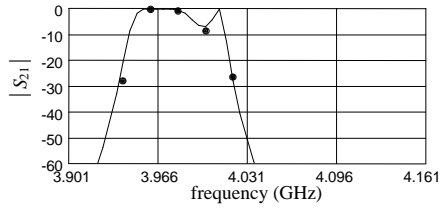
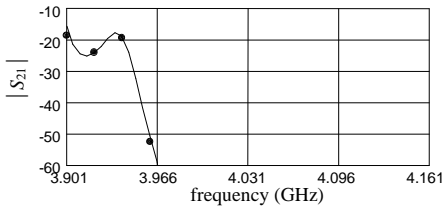
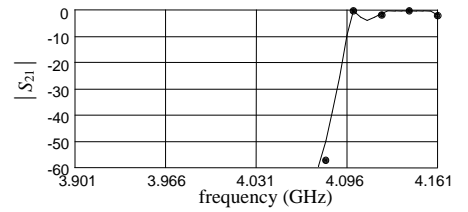
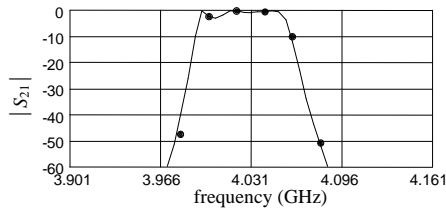
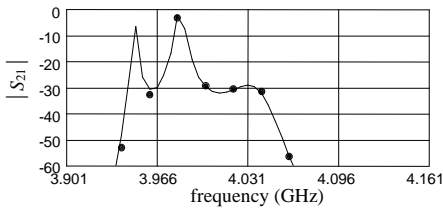
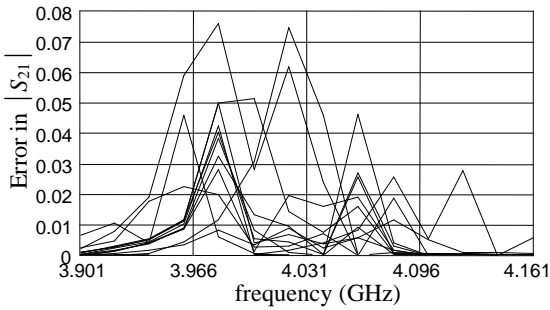
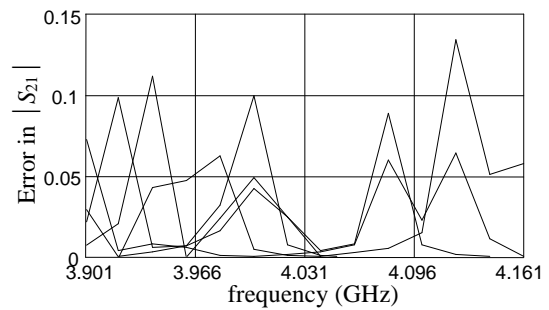


Fig. 25. Typical responses of the HTS filter using em^{TM} (\bullet) and FPSMN model ($-$) at the same three learning and three testing points as in Fig. 21.



(a)



(b)

Fig. 26. FPSMN model error w.r.t. em^{TM} : (a) in the learning set, (b) in the testing set.

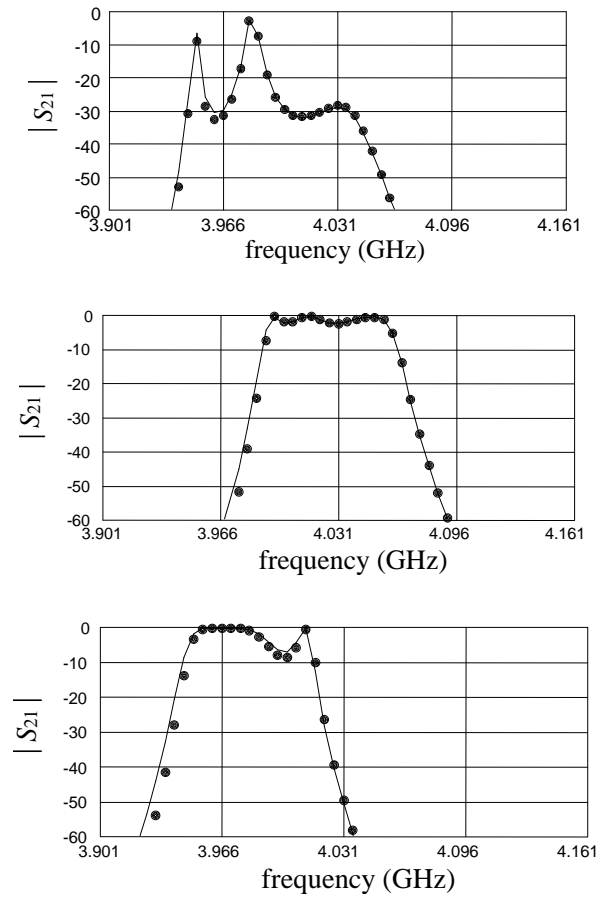


Fig. 27. Comparison between the HTS filter response using em^{TM} (•) and FPSMN model (–) at some learning and testing points using a fine frequency sweep.